Available online at www.sciencedirect.com
ScienceDirect
Journal of Solid State Chemistry 180 (2007) 2316–2322
JOURNAL OF SOLID STATE CHEMISTRY
www.elsevier.com/locate/jssc

Studies on InFeMO_4 (M = Mg, Co, Ni, Cu and Zn) compounds: Crystal structure and cation distribution

M. Matvejeff[ab]*, J. Lindén[c], M. Karppinen[a,b], H. Yamauchi[a]

[a]*Materials and Structures Laboratory, Tokyo Institute of Technology, Yokohama 226-8503, Japan*
[b]*Laboratory of Inorganic and Analytical Chemistry, Helsinki University of Technology, FI-02015 TKK, Finland*
[c]*Department of Physics, Åbo Akademi, FI-20500 Turku, Finland*

Received 31 January 2007; received in revised form 11 April 2007; accepted 12 April 2007
Available online 3 June 2007

Abstract

The crystal structure and the cation distribution in a series of InFeMO_4 compounds (M = Mg, Co, Ni, Cu and Zn) have been studied by means of X-ray powder diffraction and ^{57}Fe Mössbauer spectroscopy. The M = Mg, Co and Ni samples were confirmed to crystallize with the cubic spinel structure (space group *Fd*-3*m*), whereas the M = Cu and Zn samples adopted a hexagonal structure. For all the phases, the cation stoichiometry was found to deviate from the ideal molecular formula, InFeMO_4. The paramagnetic Mössbauer spectra of the samples were analyzed using a four-component fitting model suggested by a statistical simulation with point-charge calculation. The Mössbauer data confirmed the trivalent state for iron at both cation sites in all samples. The results from the fitting of the Mössbauer spectra were also employed in Rietveld refinement of the X-ray diffraction data for the determination of exact cation distribution. It was seen that the distribution of Fe at the A and B sites follows very closely the 1:2 ratio of the ideal formula AB_2O_4 for all samples, whereas trivalent indium was clearly seen to favor the A site and divalent M cation the B site.

Keywords: Spinel phase; Iron oxide; Mössbauer spectroscopy; Fe valence; Cation distribution

1. Introduction

A variety of oxides with the general formula AB_2O_4 adopt the crystal structure of mineral *spinel* ($MgAl_2O_4$). In the ideal spinel structure of cubic *Fd*-3*m* space group, oxygen atoms form an *fcc* lattice and divalent A cations occupy one-eighth of the tetrahedral sites with T_d symmetry and trivalent B cations occupy one-half of the octahedral sites with D_{3d} symmetry. In addition to the regular spinels, *inverse spinels* are also known. In the inverse spinel structure, half of the B cations reside in the tetrahedral positions, while equal amounts of A and B cations are found in the octahedral sites, i.e., $B_{tet}(AB)_{oct}O_4$. Between the regular and inverse spinels are so-called *mixed spinels*, $(A_{1-x}B_x)_{tet}(B_{2-x}A_x)_{oct}O_4$, in which the degree of inversion (x) is $0<x<1$.

Magnetic and transport properties of spinel oxides vary considerably depending on the identity and distribution of cations occupying the A and B sites. Hence, the spinel materials are employed in multiple applications ranging from superconductive devices and magnetic cores to switching devices and optoelectronic applications. In particular, the recent discovery of half-metallicity in magnetite (Fe_3O_4) [1] and the high spin-polarization values observed for $NiFe_2O_4$ in $La_{2/3}Sr_{1/3}O_3/SrTiO_3/NiFe_2O_4$ junctions [2] have resulted in renewed interest in the spinel oxide systems and raised hopes of finding new materials for spintronic devices. While these discoveries have triggered efforts to find ways to optimize the application potential of known systems, much work remains to be done in understanding the fundamental relations between the A- and B-site cation composition and the functional properties. A systematic approach to tailoring new phases with desired properties by careful control of the cation type and substitution level, similar to, e.g., the search for novel high-T_c superconductors, is required to fully realize the potential of this

*Corresponding author. Materials and Structures Laboratory, Tokyo Institute of Technology, Yokohama 226-8503, Japan.
E-mail address: Mikko.Matvejeff@tkk.fi (M. Matvejeff).

0022-4596/$ - see front matter © 2007 Elsevier Inc. All rights reserved.
doi:10.1016/j.jssc.2007.04.032

versatile system. Here, we describe the synthesis, crystal structures and cation distribution of various $InFeMO_4$ (M = Mg, Co, Ni, Cu and Zn) compounds which have remained poorly studied so far.

2. Crystal structures and cation and oxygen stoichiometries

Polycrystalline samples of $InFeMO_4$ were prepared with M = Mg, Co, Ni, Cu and Zn by means of solid-state synthesis using In_2O_3, Fe_2O_3 and M_3O_4 (for Co) or MO (for Mg, Ni, Cu and Zn) as starting materials. Powder mixing was carried out in an agate mortar in ethanol to ensure good homogeneity of the resulting mixture. The obtained reddish/brownish powder was pressed into pellets, which were then placed in an Al_2O_3 boat and sintered in air at temperatures ranging from 1100 to 1300 °C. In previous works involving the $InFeMO_4$ (M = Mg, Co, Ni, Cu and Zn) phases, the samples have been synthesized using stoichiometric cation compositions [3–6]. In the present study, significant amounts of impurities were observed for all M except for M = Mg and Ni when syntheses with stoichiometric cation compositions were attempted. Therefore, we carefully searched for the exact (non-stoichiometric) cation compositions for each phase that yielded single-phase samples. Details of the synthesis conditions for each M in terms of the starting cation composition and the optimal synthesis temperature are given in Table 1. Moreover, the actual cation composition of the single-phase products was determined by inductively coupled plasma (ICP-OES, Leeman Labs Inc. Prodigy High Dispersion) measurement. Results from the ICP measurements are given in Table 1. It is seen that none of the final samples exhibited exactly the ideal spinel chemical formula of $InFeMO_4$, instead the results of ICP measurements revealed loss of Co and in lesser extent of Fe and Mg during the relatively high temperature synthesis, whereas no detectable diffusion from sample to the crucible occurred for In, Cu and Zn. Therefore, in the final products, we observed lower than expected contents for Fe, Co and Mg and higher than expected contents for Ni, Cu and Zn. Although the deviations in the cation contents are small and close to the experimental error of the ICP measurement (standard deviation values of 0.5–1.3% were obtained depending on cation and sample), the results agree with the observed discoloration of the crucibles. The discoloration was strongest for the $InFeCoO_4$ sample and weaker for the other M constituents. It should also be noted that for all samples, the experimental Fe composition was systematically lower than the nominal cation composition. This can be considered as an additional confirmation for the cation diffusion, since if the difference between the nominal and observed cation compositions resulted from the experimental error(s) only, roughly half of the samples should reveal an observed iron content higher than the nominal composition. In addition, the ICP measurements confirmed that no back diffusion of Al from crucible to the sample had occurred in any of the samples.

Crystal structures of the samples were investigated by powder X-ray diffraction (Rikagu RINT-2500 V diffractometer equipped with a rotating anode) with Cu$K\alpha$ radiation on 2θ angle range 4–120°. For M = Mg, Co and Ni, the cubic (space group Fd-3m) spinel structure was confirmed (see Fig. 1); the data were used for the determination of the unit-cell parameters with the Rietveld refinement method using the program Fullprof. In the refinement, the overall cation composition was fixed to values obtained from ICP, whereas the site-specific occupancies of iron were fixed to values obtained from Mössbauer measurements as discussed later. The occupancies of In and M were fitted and the results are given in Table 2.

In the case of M = Cu and Zn, the spinel structure was not observed as is seen in the diffraction patterns in Fig. 1. Previous works have proposed a hexagonal structure with a space group R-3m for M = Cu [5], isostructural to the $n = 1$ member of the $InFeO_3(FeO)_n$ homologous series [7]. Therefore, we used the R-3m space group as a basis for the Rietveld refinement. Based on this selection, all reflections could be indexed and the obtained unit cell dimensions, $a = 3.372$ Å and $c = 24.891$ Å for M = Cu and $a = 3.323$ Å and $c = 26.129$ Å for M = Zn, were in reasonable agreement with previously reported values [5,6,8,9]. It was therefore seen that the samples were obtained essentially phase-pure. However, satisfactory fitting results could not be produced as high reliability factor values were obtained for both M = Cu and Zn samples. Therefore, further study is required to exactly determine the other structural parameters for the present M = Cu and Zn samples.

The stability of the oxygen content in terms of temperature and oxygen partial pressure was studied for all the samples by means of thermogravimetric (TG) experiments (Perkin–Elmer: Pyris 1) carried out in 1 atm O_2 and N_2 atmospheres. As the amount of sample powder

Table 1
Synthesis conditions (temperature and duration) and the nominal and actual (from ICP analysis) cation compositions of the $InFeMO_{4+\delta}$ samples

M	Nominal cation composition	Actual cation composition	Synthesis conditions
Mg	$InFeMgO_4$	$In_{1.03}Fe_{0.98}Mg_{0.99}O_4$	1300 °C, 30 h
Co	$In_{0.965}Fe_{0.965}Co_{1.070}O_4$	$In_{0.985}Fe_{0.952}Co_{1.063}O_4$	1300 °C, 4 h
Ni	$InFeNiO_4$	$InFe_{0.98}Ni_{1.02}O_4$	1300 °C, 10 h
Cu	$In_{0.990}Fe_{1.059}Cu_{0.951}O_4$	$In_{0.99}Fe_{1.05}Cu_{0.96}O_4$	1100 °C, 10 h
Zn	$In_{1.026}Fe_{0.967}Zn_{1.007}O_4$	$In_{1.034}Fe_{0.964}Zn_{1.002}O_4$	1200 °C, 72 h

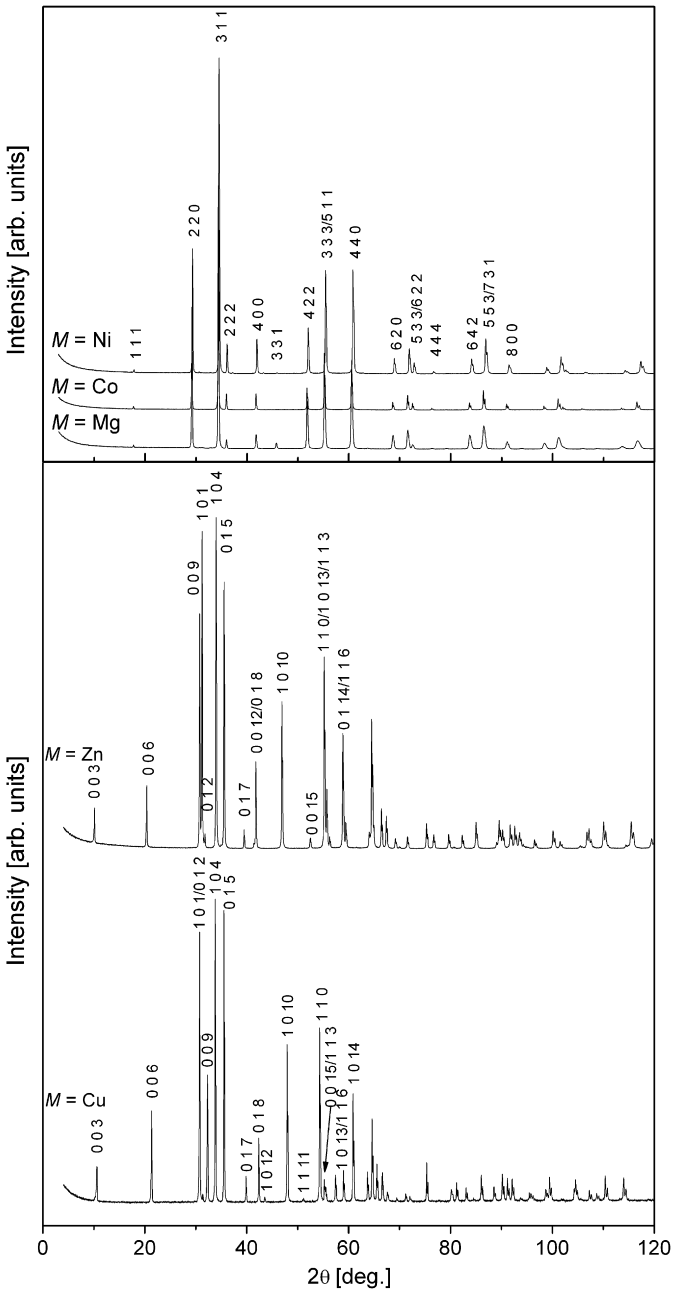

Fig. 1. X-ray diffraction patterns for InFeMO_4 samples of spinel structure for M = Mg, Co and Ni, and of hexagonal structure for M = Cu and Zn.

used in the TG measurement was small (ca. 10–15 mg) and the heating and cooling rates were slow (2 °C/min), the obtained TG curves should represent a situation close to the equilibrium state at each temperature and atmosphere. The oxygen stoichiometry of each sample was found to be highly stable in the TG measurements. Only minimal changes in weight, corresponding to less than 0.02 oxygen atoms per formula unit, were detected for the samples. The high resistance of the InFeMO_4 compounds against changes in oxygen content offers an explanation as why the samples are so sensitive to changes in the starting cation stoichiometry or sintering conditions during the preparation. For many other complex transition metal oxides

Table 2
Structural parameters of InFeMO_4, where M = Mg, Co and Ni, as obtained from Rietveld refinement and Mössbauer spectroscopy data

Structural parameters	M		
	Mg	Co	Ni
Space group	*Fd*-3*m*	*Fd*-3*m*	*Fd*-3*m*
a/b (Å)	8.63432(5)	8.63967(6)	8.60300(7)
V (Å^3)	643.70	644.89	636.72
A site composition (%) [In, Fe, M]	[66,34,0]	[54,36,10]	[58,35,7]
B site composition (%) [In, Fe, M]	[18,32,50]	[22,30,48]	[21,32,47]
Oxygen site x	0.26012	0.2625	0.2593
R_p (%)	9.57	7.47	10.4
R_{wp} (%)	11.7	9.54	12.1
χ^2	8.11	4.23	14.3

Atomic positions are 8*a* (1/8,1/8,1/8) for A site, 16*d* (1/2,1/2,1/2) for B site and 32*e* (x, x, x) for oxygen.

flexibility in terms of oxygen content can compensate for changes in the average transition metal valence occurring when the precursor cation composition and/or the synthesis conditions (temperature and atmosphere) deviate from the preferred ones. In the case of InFeMO_4, the oxygen content remains fixed, resulting in a much more limited precursor composition–synthesis condition window for phase-pure samples.

3. Site distribution and valence states of cations

The valence state and distribution of iron between the tetrahedral and octahedral sites were probed with ^{57}Fe Mössbauer measurements using a ^{57}Co source in rhodium matrix (Ritverc Company 50 mCi September 2003). To obtain a reasonable intensity of Mössbauer resonance lines, samples for each M were prepared by replacing 4.5% of regular Fe_2O_3 with ^{57}Fe-enriched Fe_2O_3. Mössbauer absorbers were made by mixing 25–30 mg of the powdered ^{57}Fe-substituted sample with fast-drying epoxy and spreading the mixture evenly on a cup made of aluminum foil with the diameter of 1.5 cm (A = 1.7 cm^2). The Mössbauer spectra for the samples exhibited only a paramagnetic signal at 300 K, except in the case of M = Ni, where a small magnetically ordered component was also detected. Due to this, the Mössbauer spectra were recorded at 300 K and additionally at 350 K for Ni, using a maximum Doppler velocity of 3.0 mm/s and were fitted with the following hyperfine parameters: the chemical isomer shift relative to α-Fe (IS), the quadrupole coupling constant (QCC), the resonance line width (Γ) and the relative intensity (I) of each component.

A representative Mössbauer spectrum is shown in Fig. 2 for M = Co. In previous works [10–13], paramagnetic Mössbauer spectra of related compounds have simply been fitted with two components, one for the A site and the other for the B site. However, it was soon revealed that the simple fitting model failed to satisfactorily explain the detailed features in the Mössbauer spectra, suggesting

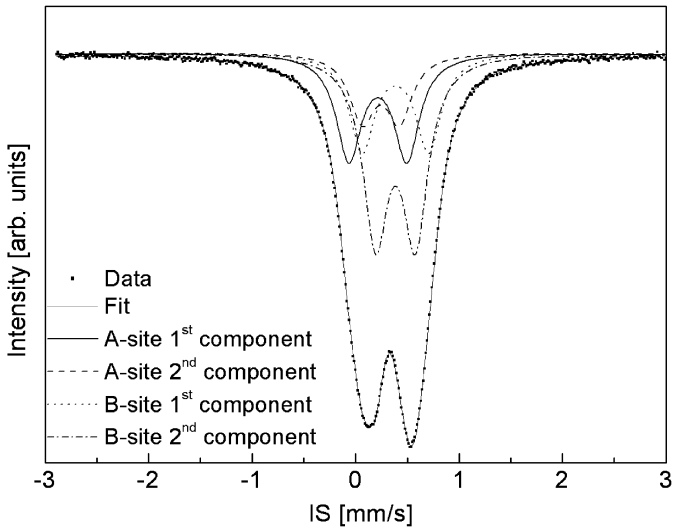

Fig. 2. Paramagnetic Mössbauer spectrum for $InFeCoO_4$.

a need for an improved model. The failure of the two-component model is expected to result from the inability of the model to describe a structure with considerable variation in the local environment around the ^{57}Fe nuclei at the A and B sites, resulting in a distribution of the QCC values. To gauge the effect of disorder on QCC, a simulation based on a point-charge model was devised for the $InFeMO_4$ (M = Mg, Co and Ni) samples with the spinel structure, whereas the simulation of the hexagonal M = Cu and Zn samples was not performed, since the site-specific cation occupancies could not be satisfactorily determined with Rietveld refinement as discussed earlier. The simulation is based on calculating the full electric field gradient (EFG) resulting from neighboring cations within a sphere constructed around the ^{57}Fe nucleus. The radius of the sphere (~7.1 Å around both sites) was chosen so as to contain a total charge as close to neutrality as possible. The neighboring cation sites surrounding the ^{57}Fe nucleus were populated randomly with site-specific occupancy values for In and M cations obtained from the Rietveld refinement of XRD data, whereas the Fe occupancy was fixed to values obtained from fitting the Mössbauer spectra with the traditional two component fitting model.

The overall probability of the cation distribution thus obtained was then calculated and the components of the EFG (V_{ij}) were obtained from the common definition of $V_{ij} = \sum_k (q_k/4\pi\varepsilon_0)((1/r_k^5)(3x_i x_j - \delta_{ij} r_k^2))$ [14], where k is an index running over all neighboring lattice sites within the sphere, q_k, x_i and x_j are the charge and coordinates of the atoms at the neighboring lattice sites and δ_{ij} is the Kronecker delta. The resulting matrix was diagonalized and the values of V_{zz} and η were extracted. V_{zz} was defined as the largest diagonal term of the matrix and $\eta = (|V_{yy}| - |V_{xx}|)/|V_{zz}|$. The value of quadrupole coupling constant was then obtained as $QCC = eQV_{zz}(1+\eta^2/3)^{1/2}$.

In order to make comparison with the measured values, the simulated values were multiplied with the so-called Sternheimer antishielding factor $(1-\gamma_\infty)$ [14]. We also note that since the simulated values concern trivalent Fe atoms, the valence contribution to the quadrupole coupling constant is zero. The following values were used for the quadrupole moment and antishielding factor: $Q = 0.15$ barn, $(1-\gamma_\infty) = 12.035$ [15,16]. It is also customary to give the quadrupole coupling constant in velocity units by multiplying it with the Doppler factor c/E_γ, where c is the speed of light and E_γ is the energy of the Mössbauer quantum (14.37 keV), leading to the final expression of $c/E_\gamma(1-\gamma_\infty)eQV_{zz}(1+\eta^2/3)^{1/2}$ for the simulated quadrupole coupling constant (simulated QCC).

To simulate the effect of structural disorder, a large number $(1-2\times10^6)$ of local cation environments were randomly created for both sites, each with their own probability and simulated QCC values. In the simulation, it was observed that only the neighboring cations contributed to the value of simulated QCC at both sites, while the contribution from neighboring oxygen atoms was zero. As the closest sites contributing to the QCC were outside the coordination polyhedron formed by oxygen atoms, the point-charge model used in this simulation could be expected to be reasonably accurate.

The simulated QCC and probability pairs were gathered and plotted in a histogram drawn by dividing the interval between the smallest and the largest simulated QCC values in approximately 100 subintervals (see Fig. 3). It was seen that for each sample, the histogram for the B site clearly consists of two main components. In addition, small changes resulting from the M cation substitution are observed. A small hump is seen in each histogram at low QCC values. At high QCC values, a satellite peak is observed for M = Mg, whereas for M = Co and Ni, a shoulder is observed for the main peak. These differences are expected to result from the changes in the unit-cell dimensions (neighboring cation distances) and variations in the ratio of divalent/trivalent cations in neighboring sites. However, these changes are too small to be individually detected in the experimental Mössbauer spectra, although the combined effect is expected to manifest as a small variation in the observed values of the resonance line widths. It should also be noted that despite the small differences in the fine structure of histograms, the results clearly suggest that the paramagnetic Mössbauer spectra of the $InFeMO_4$ spinel-type compounds should be fitted using two components for the octahedral B site with unequal QCC values, instead of only one component.

On the other hand, similar histograms for the tetrahedral A site for all samples exhibited only a broad distribution (see Fig. 4). It is expected that the current model cannot fully describe the structural disorder around the tetrahedral site, such as the deviation of oxygen atoms from their ideal positions, resulting in too small variation in the calculated values of EFG and a broad peak for distribution function instead of two distinct components as seen for the octahedral site. To test the validity of this assumption, the experimental Mössbauer data for the $InFeMO_4$

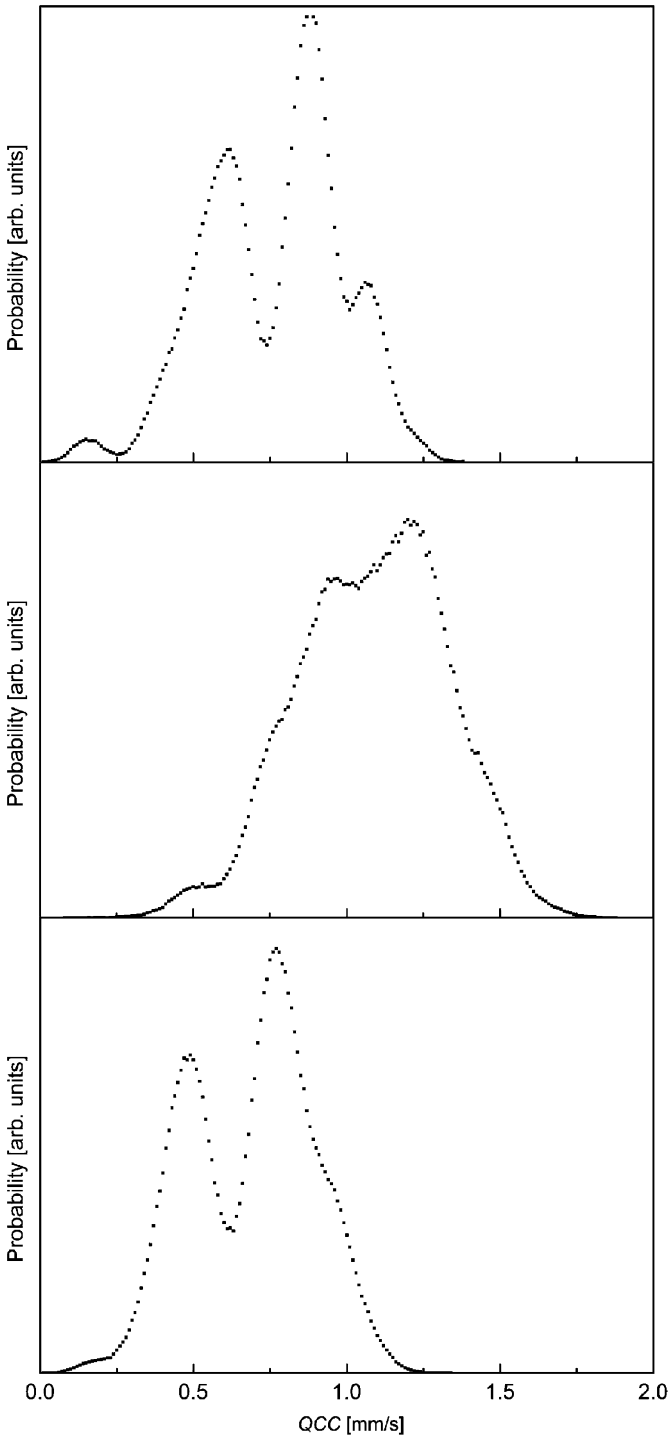

Fig. 3. Probability vs. QCC histogram for B site of InFeMO$_4$ (M = Mg, Co and Ni).

samples with M = Mg, Co and Ni were fitted with both the three-component (one component for tetrahedral, two for octahedral) and the four-component (two for both sites) models, with the four-component model producing consistently better fitting results for all samples.

Based on the results from the simulations, a new fitting model for the InFeMO$_4$ samples with spinel structure is now proposed, based on a four-component fitting method

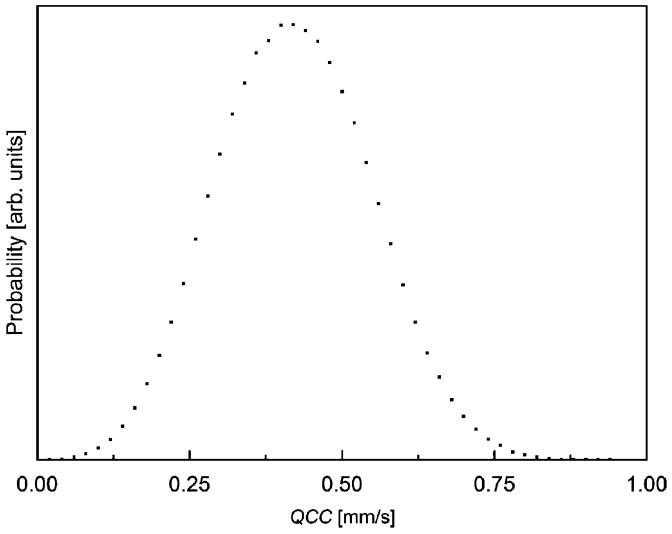

Fig. 4. Probability vs. QCC histogram for A site of InFeCoO$_4$.

with two components for tetrahedral and octahedral sites each (see Fig. 2). The values of the fitted hyperfine parameters are gathered in Table 3. The IS values confirm that iron is in trivalent state at both sites in all samples. The somewhat lower IS value for the tetrahedral site in all samples is due to a higher degree of covalency. The differences in the QCC values between the octahedral and tetrahedral sites result from the differences in the distances and the number and location of the neighboring cations, whereas based on the simulation, it is expected that the oxygen atoms do not significantly contribute to the QCC on either site. Additionally, it is worth noting that the B-site values of simulated QCC (see Table 3) are in reasonable agreement with the QCC values obtained from the experimental Mössbauer spectra, especially in the case of M = Co, hence providing further confirmation for the validity of the proposed fitting scheme. The values for the A site are not compared as the simulation resulted only in one broad distribution for that site for all samples.

The distribution of iron between the A and B sites was deduced from the sum of component intensities of each site (see Table 3). Occupancy values of iron follow closely the ratio of 1:2 between tetrahedral and octahedral sites of the ideal spinel formula AB_2O_4 for all samples, whereas judging from the Rietveld refinement results the trivalent indium is clearly seen to favor the A site and divalent M cation the B site as seen in Table 2. Based on these results, it is now possible to calculate the ratio of divalent/trivalent oxidation states for M = Co and Ni in the present InFeMO$_4$ spinel samples.

Taking the charge neutrality condition into account, it can be calculated for the M = Co sample that ~6% of Co is in the trivalent state and ~94% in the divalent state as only trivalent state was confirmed for Fe from the Mössbauer data. It should be now noted that the amount of trivalent Co is much lower than the observed A-site occupancy (approximately 34% of all cobalt); therefore,

Table 3
Hyperfine parameters for $InFeMO_4$ samples obtained with fitting the Mössbauer spectra with four-component model

M	Site		Intensity (%)	IS (mm/s)	QCC (mm/s)	Simulated QCC (mm/s)
Mg	*A* site	C1A	10.6	0.173	1.296	–
		C2A	23.6	0.206	0.904	–
	B site	C1B	24.5	0.38	1.276	0.88/1.06
		C2B	41.2	0.368	0.766	0.62
Co	*A* site	C1A	23.4	0.215	1.120	–
		C2A	14.6	0.243	0.718	–
	B site	C1B	21.7	0.385	1.286	1.20
		C2B	40.3	0.386	0.766	0.94
Ni	*A* site	C1A	11.6	0.168	1.226	–
		C2A	31.3	0.225	0.756	–
	B site	C1B	18.7	0.307	1.366	0.77/0.95
		C2B	38.4	0.344	0.740	0.49
Cu	*A* site	C1A	24.3	0.207	1.164	–
		C2A	29.4	0.208	0.812	–
	B site	C1B	25.1	0.337	1.086	–
		C2B	21.2	0.334	0.782	–
Zn	*A* site	C1A	28.2	0.219	1.246	–
		C2A	27.7	0.235	0.776	–
	B site	C1B	18.9	0.322	1.320	–
		C2B	25.2	0.34	0.808	–

C1A/B and C2A/B are component 1 and component 2 for *A* and *B* sites, respectively. IS is the value of isomer shift, QCC is the value of experimentally determined quadrupole coupling constant and simulated QCC is quadrupole coupling constant obtained from point-charge simulation.

it is clear that although some trivalent Co may exist in the sample, the majority of cobalt at both sites is in the divalent state. In the case of $InFe_{0.98}Ni_{1.02}O_4$, a parallel reasoning reveals that approximately 2% of Ni is in the trivalent state. This value is also clearly lower than the observed *A*-site occupancy (35%) of Ni, which seems to indicate that the existence of the trivalent oxidation state for the *M*-cation is not the main factor determining the *A*-site occupancy of the *M* cations. Here, it should also be noted that the cation distribution values obtained for the current samples are in contrast with the previous reports in case of $InFeCoO_4$ and $InFeMgO_4$. In the case of $InFeCoO_4$, Sakai et al. [17] have previously suggested a cation distribution model where Fe is located at the *A* site only and the *B* site is occupied by Co and In. However, no characterization results validating the proposed model were presented and the model is also contradicted by the previous Mössbauer study of Gerardin et al. [3] which proposes a very similar distribution for iron as observed in the present study.

In the case of the $InFeMgO_4$ phase, the previous Mössbauer study of Kirichok and Antoshchuk [18] confirms the presently observed *A*-site preference for In, although in contrast to the current results, a small amount of Mg is also reported to reside at the *A* site. However, the difference between the presently observed and previously reported Mg distributions is relatively small and is tentatively attributed either to the difference in the employed synthesis method or the exact chemical composition of the sample. In addition, the observed Fe distribution for the current $InFeMgO_4$ sample is in good agreement with the previous Mössbauer study of Gerardin et al. [3]. The Fe distribution reported for $InFeNiO_4$ in the same study is in reasonable agreement with the presently reported values. The observed differences are of the same level as those observed in the case of Mg occupancy and are expected to result from the similar differences in preparation methods. In addition, it can also be argued that the different (two-component) fitting model employed in the Mössbauer study of Gerardin et al. is one of the reasons contributing to the observed difference in cation distribution.

4. Conclusions

The crystal structure and the cation distribution in a series of $InFeMO_4$ compounds (where $M = Mg$, Co, Ni, Cu and Zn) have been studied. The $M = Mg$, Co and Ni samples were confirmed to crystallize with the cubic spinel structure, whereas the $M = Cu$ and Zn samples were found to be of a hexagonal structure. It was shown that only the $M = Mg$ and Ni samples can be obtained in phase-pure form from stoichiometric precursor composition and that for all phases the final cation stoichiometry deviates from the ideal chemical formula, $InFeMO_4$. The oxygen stoichiometry of the phases was confirmed to be highly stable.

The valence state of iron was probed for all *M* constituents with ^{57}Fe Mössbauer measurements at temperatures

where the samples exhibited only paramagnetic signal. It was revealed that the traditional fitting model consisting of one component for each of the two sites, A and B, produced unsatisfactory results and a simulation with point charge model was devised to gauge the effect of structural disorder on quadrupole coupling constant. Based on the simulation results, an improved model with two components for both the sites, A and B, was suggested and employed in fitting the paramagnetic Mössbauer spectra of the $InFeMO_4$ samples. It also needs to be emphasized that while the validity of the proposed fitting scheme has been confirmed only for the present $InFeMO_4$ samples with $M = Mg$, Co, Ni, Cu and Zn, it is reasonable to expect that similar improvements would be obtained by employing the new model in fitting of any spinel samples with a similar degree of variation in local environment around the Fe site.

From the Mössbauer data, it was confirmed that iron is in trivalent state at both sites in all samples. Additionally, the occupancy ratio of Fe at both sites was studied and the cation distribution of each sample was determined by means of Rietveld refinement of X-ray diffraction data. It was seen that the distribution of Fe among the A and B sites follows very closely the 1:2 ratio of the ideal formula AB_2O_4 for all samples, whereas trivalent indium is clearly seen to favor the A site and divalent M cation the B site.

Acknowledgments

This work was supported by a Grant-in-aid for Scientific Research (No. 15206002) from the Japan Society for the Promotion of Science, by an International Collaborative Research Grant of MSL, Tokyo Tech, and also by Academy of Finland (Decision Nos. 110433, 114517 and 116254). M.M. thanks the Japan Society for the Promotion of Science (JSPS) for a fellowship under the Program FY 2004 JSPS Postdoctoral Fellowship for Foreign Researchers and Scandianvian–Japan Sasakawa Foundation for the financial support.

References

[1] A. Yanase, K. Siratori, J. Phys. Soc. Japan 53 (1984) 312–317.
[2] U. Luders, G. Herranz, M. Bibes, K. Bouzehouane, E. Jacquet, J.P. Contour, S. Fusil, J.F. Bobo, J. Fontcuberta, A. Barthelemy, A. Fert, J. Appl. Phys. 99 (2006) 08K301/301–308K301/303.
[3] R. Gerardin, A. Alebouyeh, J.F. Brice, O. Evrard, J.P. Sanchez, J. Solid State Chem. 76 (1988) 398–406.
[4] N. Kimizuka, T. Mohri, J. Solid State Chem. 60 (1985) 382–384.
[5] N. Kimizuka, E. Takayama, J. Solid State Chem. 53 (1984) 217–226.
[6] N. Kimizuka, T. Mohri, Y. Matsui, K. Siratori, J. Solid State Chem. 74 (1988) 98–109.
[7] K. Kato, I. Kawada, N. Kimizuka, T. Katsura, Z. Kristallogr., Kristallgeom., Kristallphys., Kristallchem. 141 (1975) 314–319.
[8] N. Kimizuka, T. Mohri, J. Solid State Chem. 78 (1989) 98–107.
[9] N. Kimizuka, M. Isobe, M. Nakamura, T. Mohri, J. Solid State Chem. 103 (1993) 394–402.
[10] S. Wha Lee, S. Yong An, C.S. Kim, J. Magn. Magn. Mater. 226–230 (2001) 1403–1405.
[11] S.J. Kim, B.R. Myoung, C.S. Kim, J. Magn. Magn. Mater. 272–276 (2004) 2161–2162.
[12] S. Ghosh, P.M.G. Nambissan, R. Bhattacharya, Phys. Lett. A 325 (2004) 301–308.
[13] A. Lakshman, P.S.V.S. Rao, K.H. Rao, Mater. Lett. 60 (2005) 7–10.
[14] P. Gütlich, Mössbauer Spectroscopy I, vol. V, Springer, Berlin, 1975.
[15] G. Martinez-Pinedo, P. Schwerdtfeger, E. Caurier, K. Langanke, W. Nazarewicz, T. Sohnel, Phys. Rev. Lett. 87 (2001) 062701–062704.
[16] Z. Su, P. Coppens, Acta Crystallogr. A 52 (1996) 748–756.
[17] Y. Sakai, N. Kimizuka, T. Mohri, N. Tsuda, J. Phys. Soc. Japan 55 (1986) 1402–1403.
[18] P.P. Kirichok, A.I. Antoshchuk, Izv. Vyssh. Uchebn. Zaved. Fiz. 20 (1977) 86–90.